Natural Resources for Human Health
eISSN: 2583-1194

Original Research

Received 15 April 2026
Revised 21 May 2026
Accepted 20 June 2026

Natural Resources for Human Health 2026, Vol. 6 (3s): 1056–1067

KEYWORDS:
Material Science Water Treatment, Nano Particles, Iron Oxide, Sustainable energy

Structural and Orthorhombic Phase Formation of Magnetic Fe3O4 Nanoparticles for Degradation of Methyl Orange Dye

Pratiksha Jadon[1]*, Shalini Sharma[2], Sampat G. Deshmukh[3], Abhilasha Sharma[4], Rupesh Gupta[5]

[1]Research Scholar, Medicaps University, Indore, 453331, India.
[2]Assistant Professor, Medicaps University, Indore, 453331, India.
[3] Assistant Professor, SKN Sinhgad College of Engineering, Pandharpur,413304 India.
[4] Sushila Devi Bansal College of Engineering, Indore, 453331, India
[5]Centre for Research Impact & Outcome, Chitkara University Institute of Engineering and Technology, Chitkara University, Rajpura, 140401, Punjab, India
jadounp0101@gmail.com[1]* shalini.sharma@medicaps.ac.in[2]
samseeraj2022@gmail.com[3], abhilasha.sharma80123@gmail.com[4]
[5]rupesh.gupta@chitkara.edu.ine
*Corresponding author at: Research Scholar, Medicaps University, Indore, 453331, India.
E-mail address: jadounp0101@gmail.com (Pratiksha Jadon)

ABSTRACT: A thriving economy and the overall growth of civilization depend on having access to pure, healthy water. Magnetite nanomaterials possess a significant surface-to-volume ratio, a high sensitivity and reactivity, substantial adsorption capacity, and facile fictionalization, rendering them appropriate for wastewater treatment applications. This study details the manufacture and characterization of well-crystallized magnetite iron oxide nanomaterials, synthesized at around 80°C. Magnetite Fe3O4 NPs were produced using the co-precipitation technique with Fe2+ and Fe3+ salts of ferric chloride and ferrous sulphate in 2:1 ratio, and characterized employing the techniques of XRD, FTIR, and ultraviolet irradiation XRD reveals presence of magnetite Fe3O4 nanoparticles with orthorhombic crystal structure possessing a standard particle dimensions of about 19nm calculated by scherrer's equation. The synthesized magnetite Fe3O4 nanoparticles will be employed as an adsorptive removal of Methyl orange dye. MO is toxic, non- biodegradable and can cause serious environmental damage if released into water. It may result diarrhea, nausea, skin irritation and exposure to high doses of methyl orange dye can be fatal. The current research revealed that magnetite Fe3O4 NPs are good adsorbent material for the elimination of organic dye (MO) from wastewater.

1. INTRODUCTION

Environmental Water pollution from modernization has made the scarcity of fresh, clean water a global issue **[1]**. The majority of the discharged pollutants are extremely hazardous and have the potential to linger in the natural world, impacting both the environment and public health. Meeting increasingly strict standards for water quality is generally jeopardized since many Conventional cleaning methods have proven inadequate in removing emerging contaminants **[2, 3]**. "Nano" derives via Greek word for "dwarf." Such kind of innovation would unequivocally benefit people and the planet, and industry, since it has demonstrated remarkable outcomes across all domains. One use involves utilizing nanomaterials for the detection, prevention, and removal of contaminants **[4]**, as well as employing nanotechnology to create environmentally friendly products **[5]**. It has the capacity to enhance the

lives of individuals broadly, particularly those with significant health issues **[6, 7]**. Interest in using Magnetite IONPs as new generation adsorbents for water treatment has grown recently as a result of the declining quality of the water. Magnetized nanoparticles are extremely helpful magnetic recording, among many other sectors. Fe_3O_4 is among the most materials for applications in medical science, biological research, and potent particles of magnetism. Nanoscale compounds have enhanced chemical and physical features due to their mesoscopic impacts, tiny item impacts, atomic dimensions, and boundary impacts, in contrast to huge-scale structures. Adsorption is now a commonly utilized technique in industrial wastewater treatment. Numerous adsorbents have been created via this procedure and used to remediate pollutants that contain pharmaceuticals, artificial colors, and metallic components. **[8-11]** It is still difficult to remove dispersed adsorbent from wastewater, nevertheless. If managed well, it permits efficient adsorbent recycling and lowers operating expenses. Ferromagnetic adsorption agents have been investigated as an effective way to remove materials from wastewater. The safeguarding of the water environment is becoming more complicated as society grows, and the needs for treatment are becoming more variable. The long-term needs of water treatment procedures cannot be met by conventional water treatment materials **[12].** Consequently, there is substantial curiosity in creating materials with multiple functions. Among these, Magnetite nanoparticle adhesion agents are thought to be a high-performance water treatment material that is both efficient and safe for the environment. Owing to its diminutive dimensions, extensive surface coverage, exceptional magnetic properties, recyclability, magnetite nano-Fe_3O_4 has garnered a lot of attention. It also possesses the qualities of being biocompatible and non-toxic **[13].** The synthesis process often affects the micron-sized magnet size, shape, size distribution, and magnetic characteristics. Co-precipitation of iron minerals, micro-emulsion hydrothermal production, and thermal degradation of iron antecedent are some of the techniques used to create Fe_3O_4 nanoparticles. **[14].** During the synthesis of small particles of magnetite utilizing an aqueous solution of Fe^{2+} and Fe^{3+} salts in spite of a foundation within an inert atmosphere at ambient temperature, the co-precipitation method is frequently used among them. **[15]**

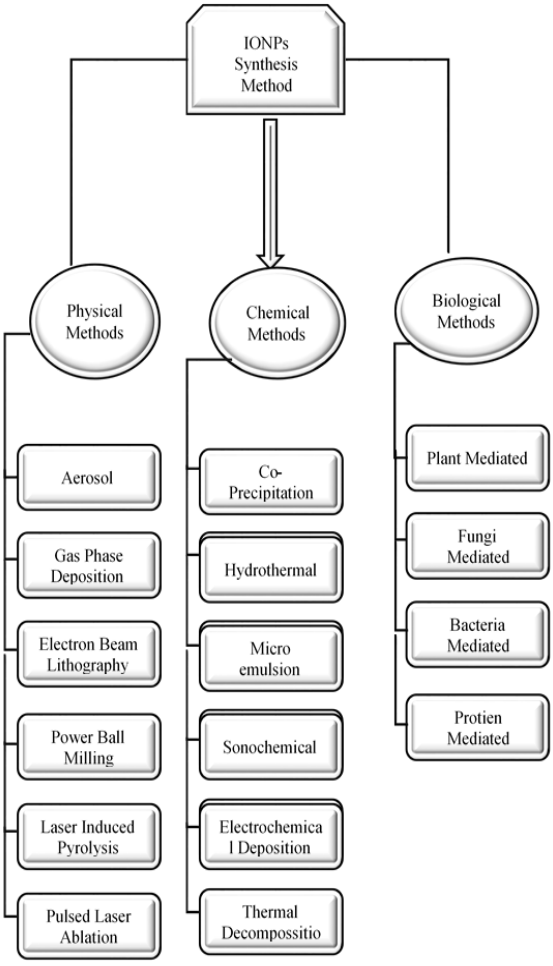

Fig.1 Different Method to Synthesis of Magnetite Fe_3O_4 nanoparticles

Magnetic characteristics of iron oxides have been employed in various usage, such as magnetized sealing and dyes, magnetic storage medium, catalysts, ferro fluids, contrast substances for MRI, and medications for cancer treatment **[16]**. These applications require nanoparticles with specified dimensions, geometries, surface attributes. Magnetism is a unique physical feature that independently facilitates the treatment of water by inducing corporal attributes of pollutants in water. The aforementioned technique, along with separation by magnets, has been extensively utilized in water purification **[17-18].** Treating and recycling both wastewater from industries and cities is vital. Over the last ten years, utilization of nanoparticles for water treatment has garnered significant focus owing to their very advantageous properties as adsorbents and for filtration purposes. Treating and recycling both wastewater from industries and cities is vital. Over the last ten years, utilization of nanoparticles for water treatment has garnered significant focus owing to their very advantageous properties as adsorbents and for filtration purposes. Moreover, Magnetic Nano particles exhibit features like a high surface area and super magnetic capabilities. Consequently, MNPs are utilized for the elimination of harmful metals Cations, endogenous materials, biotic pathogens, organic waste, nitrates, fluoride, and arsenic present in polluted water. Organic dyes constitute a significant category of pollutants extensively utilized in the fabric, plastic, medical, and various productions units. The adverse impacts of organic dyes in wastewater have emerged as a significant problem, presenting a great hazard to the ecosystem due to the extensive contamination they cause. Particles are not easily decomposed and are generally not eliminated from water by sewage treatment plants or traditional processes such as ultrafiltration, chemical, and electrochemical procedures. **[19-21]** The efficacy of nanoparticle degradation in wastewater treatment is attributable to its benefits.

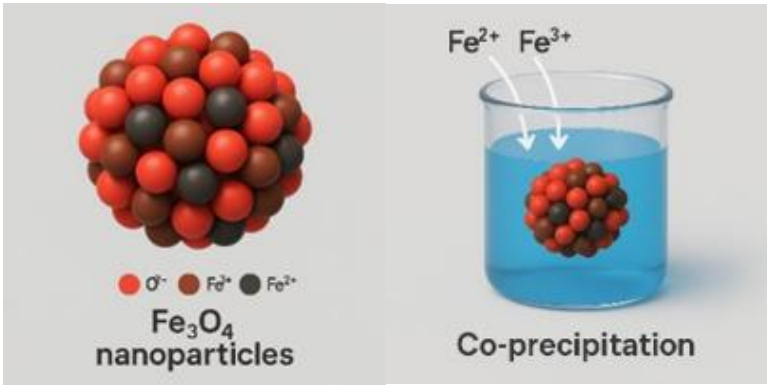

Fig.2 3D Structure of Magnetite Fe_3O_4 nanoparticles

This technology is efficient and swift for removal of pollutants from water. Specific goal of the current study was to evaluate manufactured magnetite Fe_3O_4 as adsorbent for degradation of harmful dyes, such as those found in wastewater from industry, and to synthesis magnetite Fe_3O_4 nanoparticles using an altered approach.

2. EXPERIMENTAL METHODS

2.1. Chemicals

Iron (III) chloride ($FeCl_3 \cdot 6H_2O$), iron (II) sulfate ($FeSO_4 \cdot 7H_2O$), sodium hydroxide (NH_4OH), MO dye powder were utilized in this investigation without additional purification. Deionized (DI) water was utilized throughout the whole experimental procedure for the manufacture of the adsorbent, including the methyl orange (MO) removal process.

2.2. Synthesis of Magnetite Iron Oxide Nanoparticles Co-precipitation

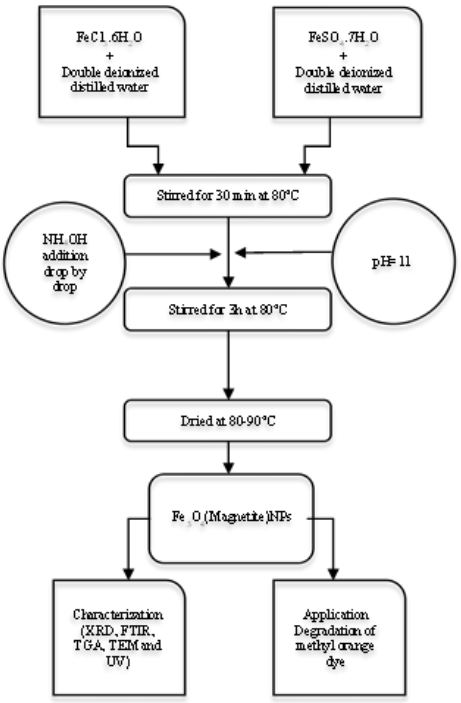

Fig.3 Process to synthesize Magnetite Fe_3O_4 nanoparticles

The Co-precipitation procedure for producing magnetite nano- Fe_3O_4 involves combining Fe^{2+} and Fe^{3+} in a 1:2 ratios, precipitating in alkaline circumstances, followed by filtration, being washed, and dried. Ammonium hydroxide was introduced as the precipitant to a combined Solution of ferrous and ferric ions in the chemical co-precipitation process, frequently utilised due to its simple nature, straightforward process, and Inexpensive and rapid-response co-precipitation techniques shown in fig. 4. The particle diameter of magnetite Fe_3O_4 can be regulated to 20 nm under suitable conditions for experimentation. **[22-23]** Using deionized water, $FeCl_3.6H_2O$, and $FeSO_4.7H_2O$, In order to manufacture magnetite nano-Fe_3O_4, the two solutions were combined and heated simultaneously. NH_4OH functioned as a precipitant in amalgamated fluid. Results demonstrated ratio of Fe^{2+}/Fe^{3+} in combined fluid significantly influenced the final product of magnetite Fe_3O_4 nanoparticles. Furthermore, the temperature influences dimensions of fragments meaning that size of magnetic Fe_3O_4 fragments rises with temperature.

Fig.4 Synthesized Magnetite Fe_3O_4 nanoparticles

2.3. Characterization

The corporeal features of produced magnetite Fe_3O_4 powder were examined utilizing several characterization techniques. X-ray diffraction investigations were performed using a Bruker D–8 Advance X-ray diffractometer with Cu Kα radiation (λ = 1.54178 Å) for compositional evaluation. The produced particles were examined using a UV-Vis spectrophotometer to confirm synthesis of magnetic Fe_3O_4 in wavelength range of 200-800 nm. FTIR spectroscopic investigation of synthesized sample was conducted using a Perkin Elmer FTIR instrument & the samples were then characterized using

thermogravimetric analysis TGA under normal atmosphere.

2.4. Techniques for Dye Elimination

Degradation experiments for the elimination of MO were conducted using the batch equilibrium method. A stock solution of MO (100 mg L^{-1}) was created by dissolving 0.1 g of MO powder in deionised water, and the necessary test solutions of MO levels were derived through repeated dilutions of the stock solution with deionized water. The batch studies were conducted using 50 mL of a MO solution at a specified concentration in a 125-mL flask. Every container included 0.05 g of adsorbent, and the combination was stirred at ambient temperature with a magnetic stirrer at a steady rate of 250 rpm for a specified duration to achieve equilibrium. After reaching adsorption equilibrium, the supernatant was isolated from the adsorbent via spinning at 5,000 rpm for 10 minutes. The quantity of MO absorption was quantified spectrophotometrically at the peak absorbance of the MO dye, λmax = 464 nm, utilizing a UV–Vis spectrophotometer. Prior to the introduction of the adsorbent, the solution's pH was adjusted to the required levels using diluted hydrochloric acid.

3. OUTCOMES AND DISCUSSIONS

3.1 Mechanism of Shape Transformation

The primary problem for scientists is the management of tiny particles structure, as numerous factors must be regulated during nanoparticle creation. This study aims to synthesise Fe_3O_4 and characterise its characteristics and

shape using a conventional approach. To achieve this objective, various precursor salts, specifically ferric chloride hexahydrate ($FeCl_3.6H_2O$) and ferrous sulphate heptahydrate ($FeSO_4.7H_2O$), along with liquids ammonia (NH_3) and sodium hydroxide (NaOH), were employed and adjusted to regulate the form of Fe_3O_4 nanoparticles through manipulation of the reaction heat. This component directly influenced the response dynamics and the rate of formation of the nanocrystals. The main procedure for synthesising Fe_3O_4 nanoparticles utilising Fe^{2+} and Fe^{3+} cations along with NH_4OH and NaOH is presented in the next equation 1.

$$Fe2+ + 2Fe3+ + 8OH- \rightarrow Fe3O4 + 4H2O \quad (1)$$

Conversely, several sequential reactions governing the form and characteristics of Fe_3O_4 nanoparticles, as documented in prior research, are encapsulated in Equations 2, 3, 4, 5, and 6:

$$Fe2+ + 2OH- \rightarrow Fe(OH)2 \quad (2)$$

$$(OH)2 + O2 \rightarrow 4FeOOH + 2H2O \quad (3)$$

$$Fe(OH)2 + 2FeOOH \rightarrow Fe3O4 + 2H2O \quad (4)$$

$$Fe3+ + 3OH- \rightarrow Fe(OH)3 \quad (5)$$

$$Fe(OH)2 + 2Fe(OH)3 \rightarrow Fe3O4 + 4H2O \quad (6)$$

3.2 X-ray Diffraction Spectroscopy (XRD)

The crystalline composition and stage purity of synthesized magnetite (Fe_3O_4) nanocrystals were examined by powder XRD. Figure 5 depicts the XRD pattern of magnetite nanocrystals. The pronounced peaks imply excellent crystallinity and great purity, while the peak broadening signifies the nanoscale dimensions of the synthesized magnetite Fe_3O_4 nanocrystals. Diffraction peaks corresponding to the planes 21.2^0 (220), 22.9^0 (031), 32.7^0 (106), 35.6^0 (333), and 58.3^0 (447) are detected for magnetite Fe_3O_4 nanoparticles. The crystal structure is orthorhombic, aligning accurately with JCPDS No. 01-076-0958. No diffraction peaks other than those of Fe_3O_4 were found, indicating the excellent purity of the produced compounds.

The formula developed by Scherrer was utilized to compute the standard crystal dimension, below.

$$D = K\lambda / (\beta \cos \theta) \quad (7)$$

The mean size of the crystallite (D) of a substance is determined from the full width at half maximum (FWHM) (β) of a peak in its X-ray diffraction (XRD) pattern, where K is an unchanged, λ represents the X-ray wavelength, and θ denotes the Bragg angle. The mean dimension of the tiny magnetite particles was ascertained to be roughly 19 nm.

Bragg's Law is articulated as $n\lambda = 2d \sin \theta$, where: n: denotes the order of reflection (an integer, often 1, 2, 3, etc.). λ: denotes

the wavelength of the X-rays. d: denotes the interplanar gap within crystal structures. θ: denotes the angle among the reflected X-rays and the crystalline planes.

The proportion of crystallinity in X-ray diffraction (XRD) study is determined by dividing the combined area of crystalline peaks by the total incorporated area beneath the XRD peaks, encompassing both crystalline and unstructured zones, and subsequently scaling by 100. The used formula ia as; % Crystallinity = (Area of crystalline peaks / Total area under the XRD curve) * 100 (table 1).

Table: 1 Structural parameter from XRD Patterns

Sample	Crystalline size (nm)	Inter planar distance (Å)	Crystallinity (%)
Pure Fe_3O_4	18.6nm	2.67Å	54.3%

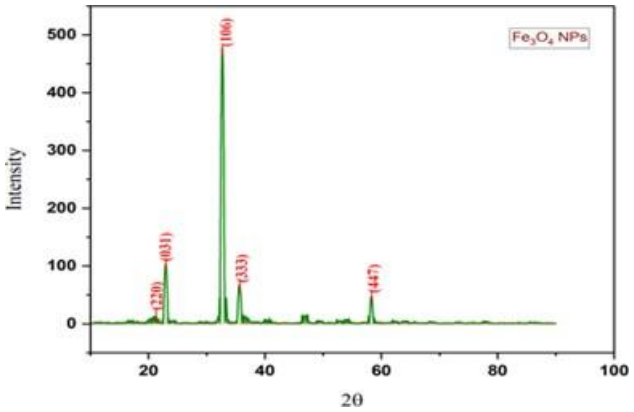

Fig.5 X-ray Diffraction Structure of Iron Oxide Nanocrystals

3.1. FTIR Experiment

FTIR analysis were performed on magnetite Fe_3O_4 nanoparticles, providing insights into the molecular bonding structure. The FTIR spectra of produced nanostructures, illustrated in Fig. 6, reveals the formation of Fe-O bands, as indicated by absorption bands at 464 cm^{-1}, 617 cm^{-1}, 798 cm^{-1}, and 893 cm^{-1}. [24-27] Additionally, peaks observed between 1111 cm-1 and 1643 cm-1, as well as between 2851 cm^{-1} and 2926 cm^{-1}, are ascribed to O-H stretching, C-H stretching, C=C stretching, C=O stretching, and C-O stretching bands, indicating the acidic medium conditions during synthesis of magnetite Fe_3O_4 nanoparticles. [28-32] The bonds detected at 3130 cm^{-1} may be featured to vibrational stretching of H_2O particles or O-H groups that are presumably present. [33]

Table: 2 Absorption Peaks from FTIR Patterns

S.no	Absorption Peak	Vibration type	References
1	462 cm^{-1} to 893 cm^{-1}	Fe-O Bands	Ref 24-27
2	1112 cm^{-1}	O-H Stretching	Ref 28
3	1401 cm^{-1}	C-H Stretching	Ref 29

4	1645 cm^{-1}	C=C Stretching	Ref 30
5	2852 cm^{-1}	C=O Stretching	Ref 31
6	2922 cm^{-1}	C-O Stretching	Ref 32

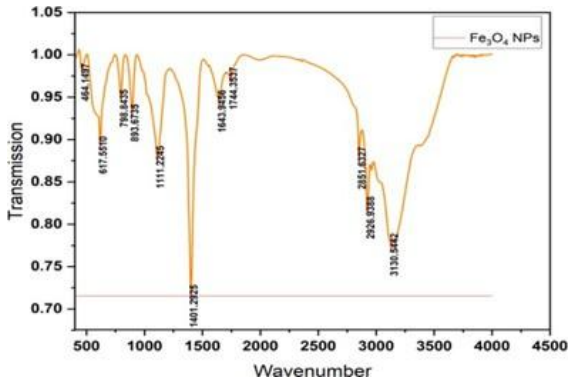

Fig.6 FTIR Peaks of Iron Oxide Nanoparticles

3.2. TGA Analysis

Thermogram displays in fig.7 a two-stage deterioration pattern within the temperature spectrum spans from 30 to 1000 °C. Initial reduction in weight of 17.93% below 300 °C can be ascribed to the vaporization and hydrolysis of immobilized and surface water from material. The second weight loss of 22.63% between 350°C to 400°C. The subsequent weight decrease of 6.27% indicates the phase shift. Consequently, the crystallization of iron oxide nanoparticles transpired at temperatures below 600 °C. Subsequently, sample weight remains nearly constant **[34]**, indicating thermal steadiness of material.

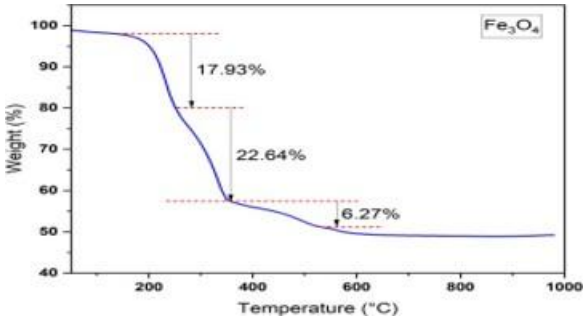

Fig.7 TGA Pattern of Iron Oxide Nanoparticles

3.3. UV-Visible Study

The visual belongings of synthesized Fe_3O_4 nanoparticles were studied using UV-Vis absorption spectroscopy. Figure 8 illustrates the optical absorption spectra of magnetite Fe_3O_4 nanoparticles, with photon wavelengths spanning from 200 to 800 nm. The typical surface plasmon absorption band seen at 338 nm indicates existence of Fe-O link in black tiny particles of magnetite generated by ferrous chloride and ferric chloride.

Natural Resources for Human Health
eISSN: 2583-1194

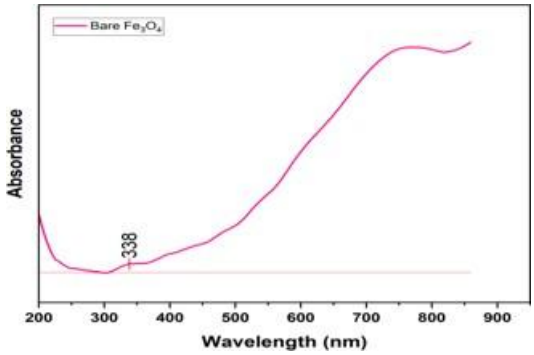

Fig. 8 UV-vis absorbance of Iron Oxide Nanoparticles

3.4. Morphological Investigations: HR-TEM Analysis

The HR-TEM analysis was performed using a JEOL 2100 instrument at an applied voltage of 180 eV. The powder sample was dispersed in ethanol solvents under ultra-sonication (15 Hz, 20 min) and mounted on carbon carbon-coated copper grid. The mounted samples were dried at room temperature overnight. The dried sample was inserted into the specimen holder to analyses the sample under high vacuum conditions. Figure 9 displays complete HR-TEM results for the shape, sizes, and crystalline features of the prepared ferrite nanomaterials. The cube monographs with uniform distribution were observed during the scanning of the samples at different areas of the loaded samples (Figure 9a), which have a 0.25 nm d-spacing, indicating the diffraction plane of (311), (Figure 9b). Whereas the selected area electron diffraction (SAED) pattern indicates its crystalline nature, having different diffraction angles, which also match with the XRD peaks. However, (Figure 9d) shows an average particle size of 10.5 nm for the synthesized cubic γ- Fe_3O_4 nanoparticles, calculated by considering more than 40 particles by ImageJ software.

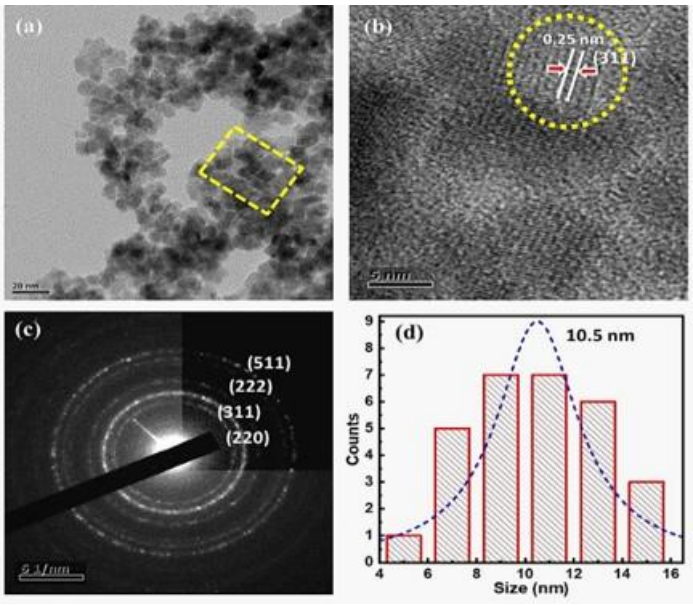

Fig.9 HR-TEM of γ- Fe_3O_4; (a) Monograph of γ- Fe_3O_4 (b) HR images of γ- Fe_3O_4 (c) SAED pattern, (d) Average particle size of γ- Fe_3O_4

3.5. Adsorption Kinetic Investigation

Kinetic investigations are essential to understand the adsorption activities, including rate of adsorption, chemical reactions, and controlled paths. Mainly, three chemical kinetic models were performed, like Pseudo first order (PFO), Pseudo second order (PSO), and intra-particle diffusion (IPD), to comprehend the adsorption procedure of as-synthesized ferrite nano sorbent.

Natural Resources for Human Health
eISSN: 2583-1194

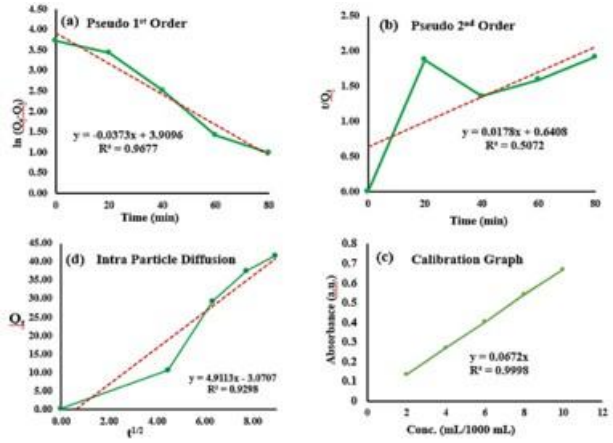

Fig.10 Kinetics of Fe_3O_4 nanosorbent; (a) Pseudo 1st order, (b) Pseudo 2nd order, (c) Intra particle diffusion.

Equations (1)–(3), signify the linear equation methods for the PFO, PSO, and IPD, individually, offered to calculate the kinetic parameters

$$\ln (Q_e\text{-}Q_t) = \text{In } Q_e - k_1 t/2.303 \quad (8)$$

Here, Qe and Qt are denote to the quantities of MO adsorbed (mg/g) and t for time (min), singly; k1 (min-1) is the rate constant.

$$t/Qt = 1/K2^* Q2e + 1/Qe \quad (9)$$

k2 is the rate constant (g/mg. min) for the pseudo-second-order kinetics.

$$Qt = kidT1/2 + C \quad (10)$$

Where, kid denotes the rate constant of intra-particle diffusion (mg/g. min3/2) and the standards of C (mg/g) represent the boundary thickness. The results indicate, MO adsorbs on nano sorbent/catalysts over physisorption as a rate-limiting stage, followed by electrostatic attractions. To recognize the interaction among positively charged nano-sorbents and negatively charged MOs, an electrostatic interface. Mechanically negative spots of the MB molecule cooperate with the positive sets of the as-synthesized ferrite absorbents. Enhancing the adsorption capacity on the external open surfaces of the applied ferrite nano catalysts.

Table: 3 Kinetics parameters for Fe_3O_4 nanosorbent

S. No.	Kinetics	Parameters	MO
1	Pseudo First Order	Q_e(mg/g)	49.88
		k1(min^{-1})	$4.6*10^{-4}$
		R^2	0.97
2	Pseudo-Second Order	Q_e(mg/g)	56.18
		k2(g/mg. Min)	$4.95*10^{-4}$
		R^2	0.5
3	Intra Particle diffusion	k_{id}(mg/g. $min^{3/2}$)	4.91
		C(mg/g)	3.07
		R^2	o.93

Table 3 demonstrates the kinetic constraints of the nano sorbents for methyl orange (MB) dye. The maximum R^2 value associated with PFO is closer to agreement than the PSO and IPD models (Fig. 10). The iron atoms among the positively charged surfaces of the nano sorbent with negatively charged MOs are the key factor to induce the adsorption of MO.

3.6. Effect of Contact Time on Dye Degradation

To investigate the impact of contact duration, a magnetite Fe_3O_4 nanoparticle dose of 0.05 g was applied to a 100 mg L^{-1} starting concentration of MO solution across several time intervals. The reaction time is an essential aspect of the depreciation response as it influences the efficiency of eliminating procedure. A limited timeframe will result in an incomplete reaction, hence diminishing the effectiveness of pollutant breakdown. Conversely, if it is excessively lengthy, it will result in superfluous waste. A number of studies were done at several durations, ranging from 20 to 80 minutes for MO (Fig. 11). The effectiveness of MO removal exhibited an upward trend throughout the initial 60 minutes. The efficacy of MO degradation was 7.1% in the initial 20 minutes, increasing to 50%, 69.6%, and 80.3% after 40, 60, and 80 minutes, respectively.

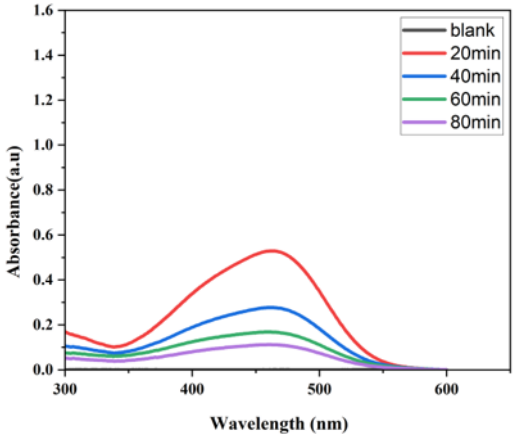

Fig.11 UV-vis absorption spectra of MO solutions for diverse contact time

Table 4. Percentage Dye Degradation at different contact time.

TIME (min)	Absorbance (nm)	Removal Percentage
20 min	0.52	7.10%
40 min	0.28	50%
60 min	0.17	69.60%
80 min	0.11	80.30%

4. CONCLUSION

This paper presents a straightforward synthesis approach for crystalline magnetite Fe_3O_4 nanostructures in response to the substantial need for wastewater treatment in factories. Nanotechnology, namely Iron Oxide Nanoparticles (IONPs), positively impacts multiple domains of environmental engineering. They can undoubtedly offer answers for mitigating pollution by regulating the morphology and dimensions of materials at the microscopic level. The remarkable characteristics

of nanomaterials, along with current economical purification technology, present significant potential to transform water and wastewater treatment. These magnetic nanomaterials possess the capacity to absorb significant quantities of contaminants or catalyze reactions at an accelerated rate. UV/visible spectroscopy studies have validated the rapid degradation behavior of Magnetite Fe_3O_4 nanoparticles. The adsorbent Fe_3O_4 nanoparticles were evaluated based on contact time. The elimination efficiency of MO was successfully predicted at different contact time and it confirms the percentage degradation of MO decreases with increasing contact time.

REFERENCES

[1] Li, Xue-Mei, Xu, Gaojie, Liu, Yue, "Magnetic Fe_3O_4 Nanoparticles: Synthesis and Application in Water Treatment" Nanoscience & Nanotechnology-Asia (14-24) Volume 1- 2011

[2] Rosa, Eliane, Fascineli, Maria Luiza, Silva, Izabel, Rodrigues, Marcelo, Chaker, Juliano, Moya, Sergio, Campos, Alex, Sousa, Marcelo, "Carbon nitride nanosheets magnetically decorated with Fe_3O_4 nanoparticles by homogeneous precipitation: Adsorption-photocatalytic performance and acute toxicity assessment" JO Environmental Nanotechnology Monitoring & Management, Volume16 (2021)

[3] Rodriguez-Narvaez, O.M., Peralta-Hernandez, J.M., Goonetilleke, A., Bandala, E.R., 2017. Treatment technologies for emerging contaminants in water: a review. Chem. Eng. J. 323, 361–380.

[4] Pankaj Ramnani Nuvia M, Saucedo Ashok Mulchandani. Carbon nanomaterial–based electrochemical biosensors for label–free sensing of environmental pollutants. *Chemosphere*. 2016;143:85–98.

[5] Arun G, Ingale, Chaudhari AN. Biogenic Synthesis of Nano particles and Potential Applications: An Eco Friendly Approach. *J Nanomed Nanotechol*; 2013.

[6] Mark E Davis, Zhuo (Georgia) Chen**,** Dong M Shin. Nano particle therapeutics: an emerging treatment modality for cancer. *Nanoscience and Technology*. 2009;239–250.

[7] Franck Furno Kelly S, Morley Ben Wong Barry L**,** Sharp Polly L. et al. Silver nano particles and polymeric medical devices: a new approach to prevention of infection? *Journal of Antimicrobial Chemotherapy*. 2004;54(6):1019–1024.

[8] Salem, I.A.; Salem, M.A.; El-Ghobashy, M.A. The dual role of ZnO nanoparticles for efficient capture of heavy metals and Acid blue 92 from water. *J. Mol. Liquids* 2017, *248*, 527–538. [CrossRef]

[9] Iannazzo, D.; Pistone, A.; Ziccarelli, I.; Espro, C.; Galvaqno, S.; Giofré, S.V.; Romeo, R.; Cicero, N.; Bua, G.D.; Lanza, G.; et al. Removal of heavy metal ions from wastewaters using dendrimer-functionalized multi-walled carbon nanotubes. *Environ. Sci. Pollut. Res.* 2017, *24*, 14735–14747. [CrossRef] [PubMed]

[10] Chaudhary, S.; Sharma, J.; Kaith, B.S.; Yadav, S.; Sharma, A.K.; Aayushi, G. Gum xanthan-psyllium-clpoly (acrylic acid-co-itaconic acid) based adsorbent for effective removal of cationic and anionic dyes: Adsorption isotherms, kinetics and thermodynamic studies. *Ecotoxicol. Environ. Saf.* **2018**, *149*, 150–158. [CrossRef] [PubMed

[11] Islam, M.T.; Hernandez, C.; Ahsan, M.A.; Pardo, A.; Wang, H.; Noveron, J.C. Sulfonated resorcinolformaldehyde microspheres as high-capacity regenerable adsorbent for the removal of organic dyes from water. *J. Environ. Chem. Eng.* 2017, *5*, 5270–5279. [CrossRef]

[12] Zhan H, Bian Y, Yuan Q, Ren B, Hursthouse A, Zhu G. "Preparation and Potential Applications of Super Paramagnetic Nano-Fe_3O_4" *Processes* 6, no. 4 (6-22) 2018

[13] Lu, F.; Astruc, D. Nanomaterials for removal of toxic elements from water. *Coord. Chem. Rev.* 2018, *356*, 147–164.

[14] G. S. Demirer, A. C. Okur and S. Kizilel, *J. Mater. Chem. B*, **3**, 7831 (2015),

[15] T. Ahn, J.H. Kim, H.-M. Yang, J.W. Lee and J.-K. Kim,*J. Phys. Chem. C*, 116, 6069 (2012),

[16] Luiz CA, Oliveira Rachel, Rios VRA, et al. *Activated carbon/iron oxide magnetic composites for the adsorption of contaminants in water, Carbon*. USA. 2002;40(12): 2177–2183.

[17] Teja AS, Koh PY. *Progress in Crystal Growth and Characterization of Materials*. USA. 2009;55: 22–45.

[18] Ming Hua, Shujuan Zhang, Bingcai Pan, et al. Heavy metal removal from water/wastewater by nano sized metal oxides. *Journal of Hazardous Materials*. 2012;211–212:317–331.

[19] Subha V, Divya K, Gayathri S, et al. Applications of iron oxide nano composite in waste water treatment–dye decolourisation and anti–microbial activity. *MOJ Drug Des Develop Ther.* 2018;2(5):178–184.

[20] Fuskele, V.; Sarviya, R.M. Recent developments in Nanoparticles Synthesis, Preparation and Stability of Nanofluids. *Mater. Today Proc.* 2017, *4*, 4049–4060.

[21] Meng, H.; Zhang, Z.; Zhao, F.; Qiu, T.; Yang, J. Orthogonal optimization design for preparation of Fe_3O_4 nanoparticles via chemical coprecipitation. *Appl. Surf. Sci.* **2013**, *280*, 679–685.

[22] Díaz-Ufano, Carlos Gallo-Cordova, Alvaro Santiandreu, Lucia Veintemillas-Verdaguer, Sabino Sáez-Puche, Regino Fernández, María Morales, Maria del Puerto "Maximizing the Adsorption Capacity of Iron Oxide Nanocatalysts for the Degradation of Organic Dyes" Journal of Colloids and Surfaces A: Physicochemical and Engineering Aspects,Vol-658,(2022)

[23] Yan Weia , Bing Hanb , Xiaoyang Hua , Yuanhua Linc , Xinzhi Wangd , Xuliang Denga , "Synthesis of Fe_3O_4 nanoparticles and their magnetic properties" Chinese Materials Conference, Procedia Engineering 27 (**2012**) 632 – 637

[24] H. M. Yusoff, M. N. Salimi, M. F. Jamlos & A. Yusoff, "Synthesis and characterization of biocompatible Fe_3O_4 nanoparticles at different pH Synthesis and Characterization of Biocompatible Fe_3O_4 Nanoparticles at Different pH," AIP Conf. Proc., 1835 (2017) 20010– 20004.

[25] O. M. Lemine, *et al.,* "Sol–gel synthesis of 8nm magnetite (Fe3O4) nanoparticles and their magnetic properties," Superlattices Microstruct., 52, 4 (2012) 793–799.

[26] M. Bhaumik, A. Maity & V. K. Gupta, "Synthesis and characterization of Fe 0 /TiO 2 nanocomposites for ultrasound assisted enhanced catalytic degradation of reactive black 5 in aqueous solutions," J. Colloid Interface Sci., 506 (2017) 403–414.

[27] M. Aghazadeh & F. Aghazadeh, "Improve Synthesis of Iron Oxide Nanorode with Hydrothermal Method," 74 (2013) 67–74.

[28] Z. Jin, e*t al.,* "Enhanced magnetic and electrochemical properties of one-step synthesized PANI-Fe3O4 composite nanomaterial by a novel green solvothermal method," J. Alloys Compd., **695** (2017) 1807–1812.

[29] H. N. Azlina, J. N. Hasnidawani, H. Norita & S. N. Surip, "Synthesis of SiO $_2$ Nanostructures Using Sol-Gel Method," Acta Phys. Pol. A, 129, 4 (2016) 842–844.

[30] S. Shafiee, O. Akhavan, H. Hatami & P. Hoseinkhani, "Sol-gel synthesis of thermoluminescent Cd-doped ZnTe nanoparticles," Indian J. Pure Appl. Phys., **53**, 12 (2015) 804–807.

[31] Z. I. Takai, M. K. Mustafa, and S. Asman, "Preparation of high performance conductive polyaniline magnetite (PANI/Fe_3O_4) Nanocomposites by Sol-Gel Method," *Asian J. Chem.*, vol. 30, no. 12, (2018) 2625-2630.

[32] M. Bilton, S. J. Milne & A. P. Brown, "Comparison of Hydrothermal and Sol-Gel Synthesis of Nano-Particulate Hydroxyapatite by Characterisation at the Bulk and Particle Level," Open J. Inorg. Non-metallic Mater., **2**, 1 (2012) 1–10.

[33] M. Jamal, M. Z. Noh, S. Al-juboor, M. Haziman, B. Wan, and Z. Ibrahim, "Mechanical Properties of the Concrete Containing Porcelain Waste as Sand," vol. **7**, (2018) pp. 180–184

[34] Li, G.S. and Smith, R.L., *Mater. Res. Bull.*, 2002, vol. 37, p. 949 PROTECTION OF METALS AND PHYSICAL CHEMISTRY Bulk and Particle Level," Open J. Inorg. Non-metallic Mater., 2, 1 (2012) 1–10.